

Enhancement of Antitumor Properties of rhTRAIL by Affinity Increase toward Its Death Receptors[†]

Carlos R. Reis,^{‡,§} Almer M. van der Sloot,^{‡,||} Eva Szegezdi,^{‡,⊥} Alessandro Natoni,[⊥] Vicente Tur,^{||}
Robbert H. Cool,^{§,¶} Afshin Samali,[⊥] Luis Serrano,[△] and Wim J. Quax^{*,§}

Department of Pharmaceutical Biology, University of Groningen, Antonius Deusinglaan 1, 9713 AV, Groningen, The Netherlands, Centre for Genomic Regulation, CRG-EMBL Systems Biology Unit, Dr. Aiguader 88, 08003, Barcelona, Spain, Department of Biochemistry and National Centre for Biomedical Engineering Science, National University of Ireland, Galway, Ireland, Triskel Therapeutics BV, Antonius Deusinglaan 1, 9713 AV, Groningen, The Netherlands, and Institució Catalana de Recerca i Estudis Avançats (ICREA), Centre for Genomic Regulation (CRG), EMBL/CRG Systems Biology Research Unit, Universitat Pompeu Fabra, Dr. Aiguader 88, 08003 Barcelona, Spain

Received October 14, 2008; Revised Manuscript Received January 8, 2009

ABSTRACT: Tumour necrosis factor-related apoptosis-inducing ligand (TRAIL) is a potent and selective inducer of apoptosis in various tumor types, raising enthusiasm for TRAIL as a potential anticancer agent. TRAIL-induced apoptosis is mediated by death receptors 4 (DR4) and DR5. The design of rhTRAIL variants either with improved affinity or selectivity toward one or both death-inducing receptors is thought to enhance the therapeutical potential of TRAIL. Here we demonstrate that a single amino acid mutation at the position of glycine 131 to lysine or arginine in wild-type rhTRAIL significantly improved the affinity of rhTRAIL toward its death receptors, with the highest affinity increase observed for the DR4 receptor. These variants were able to induce higher *in vitro* levels of apoptosis in cancer cells responsive to only DR4 or to both death receptors and could therefore increase the potential use of rhTRAIL as an anticancer therapeutic agent.

Targeting and activation of death receptors belonging to the tumor necrosis factor (TNF)¹ receptor family open a window to a unique therapeutic strategy by extrinsically inducing p53-independent apoptosis in cancer cells (1). Tumor necrosis factor (TNF) related apoptosis-inducing ligand (TRAIL) is attracting great interest as a potential anticancer therapeutic agent because of its ability to selectively trigger receptor-mediated apoptosis in cancer cells but not in normal cells (2, 3).

TRAIL is unique within the TNF ligand family as it interacts with an intricate receptor system consisting of two apoptosis-inducing or agonistic death receptors, death receptor 4 (DR4/TRAIL-R1) and death receptor 5 (DR5/TRAIL-R2), and three antagonistic or decoy receptors, decoy receptor

1 (DcR1/TRAIL-R3), decoy receptor 2 (DcR2/TRAIL-R4), and the soluble receptor osteoprotegerin (OPG) (4). Binding of TRAIL to the two apoptosis-inducing receptors (DR4 and DR5) leads to recruitment of Fas-associated death domain (FADD) (5–7), which in turn allows binding and activation of the initiator caspases-8 and -10 and induction of apoptosis (8–10). DcR1 and DcR2 lack a death domain or contain a truncated death domain, respectively. Thus, binding of TRAIL to these receptors does not induce apoptosis but could instead prevent apoptosis by sequestering available TRAIL or by interfering with the formation of a TRAIL-DR4 or -DR5 signaling complex (11). Recently, it was demonstrated that DcR2 is not merely a decoy receptor. DcR2 was shown to inhibit DR5-mediated apoptosis through ligand-independent association with DR5 via the preligand assembly domain (PLAD) (12) or to inhibit TRAIL-DR5 signaling in a ligand-dependent fashion by forming heteromeric ligand–receptor complexes (13). In addition, it is clear that the sensitivity toward this apoptosis signaling pathway is not defined solely by these components, since cell surface expression of the decoy receptors does not necessarily correlate with sensitivity of tumor cells to TRAIL (14).

Although TRAIL signals via DR4 and DR5, many studies suggest that DR5 is the primary receptor leading to apoptosis (14–17). In this light, it is perhaps expected that DR5 is the highest affinity receptor of TRAIL (18, 19). However, it has been recently shown that in primary cells from patients with chronic lymphocytic leukemia and mantle cell lymphoma the death-mediating receptor is DR4, not DR5 (20, 21).

[†] This research was partly funded by European Union Fifth Framework Program Grant QLK3-CT 2001-00498 and Sixth Framework Program Grant LSH-2005-2.2.0-2. R.H.C. was in part supported by the Technology Foundation STW, Applied Science Division of NWO, and the technology program of the Dutch Ministry of Economic Affairs.

* To whom correspondence should be addressed. E-mail: w.j.quax@rug.nl. Phone: +3150 363 2558. Fax: +3150 363 3000.

[‡] These authors contributed equally to this work.

^{||} Department of Pharmaceutical Biology, University of Groningen.

[⊥] Centre for Genomic Regulation, Barcelona.

[⊥] Department of Biochemistry, National University of Ireland.

[¶] Triskel Therapeutics BV, Groningen.

[△] Institució Catalana de Recerca i Estudis Avançats, Universitat Pompeu Fabra, Barcelona.

¹ Abbreviations: TNF, tumor necrosis factor; TRAIL, TNF-related apoptosis-inducing ligand; DR4, death receptor 4; DR5, death receptor 5; SPR, surface plasmon resonance; ELISA, enzyme-linked immunosorbent assay.

Improving a high-affinity protein–protein interaction is a challenging problem that has practical implications in the development of protein-based therapeutics. Redesign of several protein–protein interactions have been successfully accomplished by using computational protein design methods in order to modify binding characteristics (19, 22–24). Previously, we used computational protein design to generate DR5-selective TRAIL variants (19) and DR4-selective variants (25). Although DR4-selective variants showed an increase in specificity, the biological activity on DR4-responsive cells was lower when compared to wild-type rhTRAIL (25).

Designing a TRAIL variant having an increased binding affinity toward DR4 and unchanged (or increased) affinity toward DR5 could therefore be of therapeutic interest for TRAIL-sensitive cancer cells. Such a mutant would not differentiate between DR4- and DR5-sensitive tumor cells, allowing treatment of a broader range of cancer cells. In order to improve the efficiency of rhTRAIL variants mediating apoptosis via DR4, we set out to improve the affinity for DR4 without emphasizing the selectivity aspect. Here we demonstrate that such an approach is feasible, having designed TRAIL variants containing a single mutation leading to an improved affinity for both DR4 and DR5. Replacement of glycine 131 to lysine or arginine was sufficient to increase the death-inducing potency of rhTRAIL, which led to a significant improvement in biological activity.

EXPERIMENTAL PROCEDURES

All reagents were of analytical grade unless specified otherwise. Isopropyl β -D-1-thiogalactoside (IPTG), ampicillin, and dithiothreitol (DTT) were purchased from Duchefa. Chromatographic columns and media were from Amersham Biosciences. Restriction enzymes used were purchased from New England Biolabs. Recombinant TRAIL-receptor Ig fusion proteins were ordered from R&D Systems. Anti-caspase-3 and anti-caspase-8 were from Cell Signaling Technology. All other chemicals were from Sigma. All buffers used in SPR and ELISA or biological activity assays were of physiological pH and ionic strength.

Modeling of TRAIL–Receptor Complexes. At present only the crystal structure of TRAIL in complex with the DR5 receptor is known. The template selected was 1D4V (26), the structure at 2.2 Å resolution and of monomeric human TRAIL in complex with the ectodomain of DR5 (TRAIL-R2) receptor. The homotrimer was generated using the protein quaternary structure server from the EBI (<http://pqs.ebi.ac.uk>), having the symmetry coordinates in the PDB file. From the sequence alignment of the different TRAIL receptors it is observed that the receptor cysteine-rich domains (CRDs) involved in the interaction with TRAIL (CRD2 and CRD3) are highly conserved, with the exception of the soluble receptor OPG. Indeed, when compared to DR5, the sequence identity of any other membrane-attached TRAIL receptor is higher than 50% in each case, and there are neither insertions nor deletions in the sequence (with the exception of a glycine deletion in the middle of the CRD3 in DcR1). In addition, all of the cysteines involved in the formation of internal disulfide bridges are conserved and share the same sequence position. Thus, it was possible to build homology models of all TRAIL receptors except for OPG.

The homology model of TRAIL-DR4 was built using the protein design capabilities of FoldX. The DR5 amino acid residues were mutated into the corresponding DR4 amino acids, and subsequently, all amino acid side chain interactions were optimized in order to accommodate TRAIL and receptor residues to their new interface.

Computational Design of the Mutants. A detailed description of the empirical force field FoldX (version 3.0) is available elsewhere (27, 28) (and at <http://foldx.crg.es>). Briefly, this force field calculates the free energy of unfolding (ΔG) of a target protein or protein complex combining the physical description of the interactions with empirical data obtained from experiments on proteins. Force field components (polar and hydrophobic solvation energies, van der Waals interactions, van der Waals clashes, H-bond energies, electrostatics in the complex and its effects on the k_{on} and backbone and side chain entropies) are calculated evaluating the properties of the structure, such as its atomic contact map, the accessibility of its atoms and residues, the backbone dihedral angles, the H-bond network, and the electrostatic network of the protein. Water molecules making two or more H-bonds with the protein are also taken into account (29).

FoldX is able to perform amino acid mutations and simultaneously accommodate the new residues and its surrounding amino acids (28). FoldX first mutates the selected position to alanine and annotates the side chain energies of the neighbor residues. Then it mutates this alanine to the selected amino acid and recalculates the side chain energies of the same neighboring residues. Those that exhibit an energy difference are then mutated to themselves to see if another rotamer will be more favorable.

This procedure was also used to reconstruct the binding interface of TRAIL in complex with the modeled DR4 receptor: In order to repair residues with bad torsion angles, residues having bad van der Waals clashes, or to build up the putative interactions between TRAIL and the modeled receptor, the most optimal amino acid conformation was chosen using rotamer substitution (see above). The crystal structure of TRAIL in complex with the DR5 receptor was also refined in this way.

Site-Directed Mutagenesis, Expression, and Purification of rhTRAIL Variants. cDNA corresponding to human soluble TRAIL (aa 114–281) was cloned in pET15b (Novagen) using *Nco*I and *Bam*HI restriction sites. Mutants were constructed by polymerase chain reaction (PCR) using the QuikChange site-directed mutagenesis (Stratagene) method. The polymerase used was *Pfu* Turbo supplied by Stratagene. Introduction of mutations was confirmed by DNA sequencing. Wild-type rhTRAIL and variants cloned into pET15b were transformed into *Escherichia coli* BL21(DE3). Homotrimeric TRAIL proteins were overproduced, and the harvested cells were resuspended in 3 mL/g of wet cells in extraction buffer [PBS, pH 8, 10% (v/v) glycerol, 7 mM β -mercaptoethanol]. Cells were disrupted using sonication, and extracts were clarified by centrifugation for 60 min at 40000g. Subsequently, the supernatant was loaded on a nickel-charged HisPrep FF 16/10 column (GE Healthcare), and wild-type TRAIL and TRAIL mutants were further purified by cation-exchange chromatography on a HiTrap SP HP column (GE Healthcare) as described before (30). Analytical gel filtration using a Hiload Superdex 75 16/60 column (GE Healthcare) (Supporting Information Figure S1),

dynamic light scattering, and nonreducing gel electrophoresis were used to confirm that wild-type TRAIL and variants were trimeric molecules, not forming higher degree aggregates and not containing interchain disulfide bridges. Purified protein solutions were flash frozen in liquid nitrogen and stored at -80°C .

Determination of Receptor Binding by Surface Plasmon Resonance. Binding experiments were performed using a surface plasmon resonance-based biosensor Biacore 3000 (Biacore AB). Research grade CM5 sensor chips, *N*-hydroxysuccinimide (NHS), *N*-ethyl-*N'*-(3-diethylaminopropyl)carbodiimide (EDC), ethanolamine hydrochloride, and standard buffers, e.g., HBS-N and HBS-EP, were purchased from the manufacturer. All of the buffers were filtered and degassed. Immobilization of DR4-Ig and DR5-Ig receptors (R&D Systems) on the sensor surface of a Biacore CM5 sensor chip was performed following a standard amine coupling procedure according to the manufacturer's instructions. Receptors were coated at a level of ~ 800 response units. Activated, coupled surfaces were then quenched of reactive sites with 1 M ethanolamine (pH 8). Reference surfaces consisted of activated CM dextran, subsequently blocked with ethanolamine. A 50 μL aliquot of TRAIL and variants was injected in 3-fold at concentrations ranging from 250 to 0.5 nM at 70 $\mu\text{L}/\text{mL}$ and at 37°C using HBS-N supplemented with 0.005% surfactant P20 (Biacore) as running and sample buffer. Binding of ligands to the receptors was monitored in real time. Between injections the receptor/sensor surface was regenerated using 1:1 10 mM glycine, 1.5 M NaCl, pH 2:ethylene glycol and a contact time of 30 s.

Determination of Receptor Binding by ELISA and Competitive ELISA Assay. To estimate the fold difference in affinity of mutants versus wild-type rhTRAIL, we used a competitive ELISA in addition to ELISA assay. Nunc maxisorb plates were coated for 2 h with DR4-Ig (100 ng per well) in 0.1 M sodium carbonate/bicarbonate buffer (pH 8.6), and the remaining binding places were subsequently blocked with 2% BSA for 1 h. After being washed for six times with Tris-buffered saline/0.5% Tween 20 (TBST) (pH 7.5), serial dilutions of soluble DR4-, DR5-, DcR1-, or DcR2-Ig (0–500 ng per well) and wild-type rhTRAIL or mutants (10 ng per well) in PBS (pH 7.4) preincubated for 1 h at room temperature were added to the wells and incubated for 1 h at room temperature. For the ELISA assay serial dilutions of wild-type rhTRAIL and variants (0–1000 ng per well) were added to the well coated with DR4-Ig and DR5-Ig and incubated at room temperature for 1 h. After being washed for six times with TBST, a 1:200 dilution of anti-TRAIL antibody (R & D Systems) was added and incubated for 1 h at room temperature, and, after being washed six times with TBST, subsequently incubated with a 1:25000 dilution of a horse radish peroxidase-conjugated swine anti-goat antibody. After being washed six times with TBST, 100 μL of 1-step Turbo TMB solution (Pierce) was added, and after 20 min, the reaction was quenched with 100 μL of 1 M sulfuric acid. The absorbance was measured at 450 nm on a microplate reader (Thermo Labsystems). Binding of rhTRAIL or variants to immobilized DR4-Ig with 0 ng per well of the soluble receptors was taken as 100%, and binding at other concentrations of soluble receptors was calculated relative to 0 ng per well of soluble receptor.

Cell Line and Treatment. Colon carcinoma Colo205 and HCT15, BxPC pancreatic carcinoma, ML-1 acute myeloid leukemia, EM-2 chronic myelogenous leukemia, and Burkitt's lymphoma BJAB cell lines were maintained in RPMI1640 medium, supplemented with 10% FBS, 50 units/mL penicillin, 5 mg/mL streptomycin, 2 mM L-glutamine, and 1 mM sodium pyruvate in a humidified incubator at 37°C and 5% CO_2 environment. HepG2 hepatocellular carcinoma cells were cultured in DMEM, with 10% FBS, 50 units/mL penicillin, 5 mg/mL streptomycin, and glutamine. Colon carcinoma SW948 cells were cultured in Leibovitz L15-RPMI 1640 (1:1) enriched with 10% FBS, 0.05 M pyruvate, 0.1 M glutamine, and 0.025% β -mercaptoethanol at 37°C in a humidified atmosphere with 5% CO_2 . Human dermal fibroblasts were grown in low glucose DMEM (Sigma) supplemented with 10% fetal calf serum, 50 units/mL penicillin, and 5 mg/mL streptomycin; human umbilical vein endothelial cells (HUVEC; PromoCell) were cultured in endothelial cell growth medium with SupplementMix (PromoCell). All cells were seeded at 50% confluency 24 h prior to treatment. Cells were cultured in a humidified atmosphere at 37°C and 5% CO_2 and treated with recombinant human TRAIL or rhTRAIL variants G131K and G131R.

Annexin V Staining. Cells were seeded the day before the experiment in 24-well plates (0.5 mL/well) for ML-1, EM-2, HCT15, BxPC, and HepG2 cell types. Wild-type rhTRAIL, G131R, or G131K (5–250 ng/mL) was added to the cells and incubated for 24 h. Cells were transferred into Eppendorf tubes and spun down. Cell pellets were resuspended in 50 μL of annexin V incubation buffer (10 mM HEPES/NaOH, pH 7.4, 140 mM NaCl, 2.5 mM CaCl_2) containing 6 μL of annexin V-fluorescein isothiocyanate (IQ Corp.) for 15 min on ice. The reaction was stopped by adding 300 μL of fresh incubation buffer, and the samples were analyzed immediately using a FACSCalibur flow cytometer (BD Biosciences). Results were expressed as percentage of annexin V-positive cells.

Cytotoxicity and Caspase Activity. BJAB, Colo205, and SW948 cells were seeded in 96-well plates the day before the experiment. Ligands (wild-type rhTRAIL and Gly-131 variants) were serially diluted in cell culture medium (1.5–100 ng/mL) and then added to each well of a 96-well tissue culture microplate (Greiner) containing cells. Mixtures were incubated for 24 h at 37°C in a humidified atmosphere containing 5% CO_2 . Subsequently, 20 μL of MTS (Promega) reagent was added. Cell viability was determined after 1 h of incubation by measuring the absorption at 490 nm on a microplate reader (Thermo Labsystems). BJAB cell lines were incubated with concentrations ranging from 1.5 to 100 ng/mL TRAIL or variants in the presence of 0.33 $\mu\text{g}/\text{mL}$ cycloheximide (Sigma) or without cycloheximide for the BJAB^{WT} cell line. Caspase activity was determined using a Caspase-Glo 3/7 assay (Promega) in a 96-well plate. SW948 colon carcinoma cells were plated in a 96-well plate and treated with wild-type rhTRAIL and Gly-131 variants (100 ng/mL) for 20 h or left untreated. The Caspase-Glo 3/7 reagent was added to wells, and luminescence was recorded at 1 h with a luminometer.

For immunoblotting, ML-1 cells were seeded in 6-well plates at the usual density. After treatment with rhTRAIL and the Gly-131 variants and pretreatment with z-VAD.fmk (Enzyme Systems Products), the cells were harvested, and

cells were used for annexin V assay, and the rest were washed once in PBS and lysed in 100 μ L of lysis buffer (1% Triton X, 10% glycerol, 150 mM NaCl, 20 mM Tris-HCl, pH 7.6). Cells were incubated on ice for 5 min and then spun down for 5 min. The supernatant was collected, and protein concentration was determined by the BCA method (Pierce). Thirty micrograms of proteins was loaded onto 12% SDS-PAGE. After electrophoresis, proteins were transferred into a polyvinylidene fluoride membrane. The membrane was blocked for 1 h at room temperature in blocking buffer (5% nonfat dry milk in PBS/0.05% Tween 20) and incubated overnight with rabbit anti-caspase-3 polyclonal antibody at 4 °C (1:500 in blocking buffer). The membrane was then washed three times for 5 min in washing buffer (PBS/0.05% Tween 20) and incubated with goat anti-rabbit IgG HRP-conjugated secondary antibody (Pierce) for 1 h at room temperature in blocking buffer. After incubation, the membrane was washed three times in washing buffer and once in PBS for 5 min. The membrane was developed using SuperSignal West Pico chemiluminescent substrate (Pierce) according to the manufacturer's instructions.

Western Blotting. For antigen detection membranes were incubated with antibodies to actin (1:500; Sigma) and caspase-3 and -8 (1:500; Cell Signaling Technologies) overnight at 4 °C followed by 2 h incubation at room temperature with appropriate secondary antibodies (1:5000; Pierce). Protein bands were visualized using Supersignal Ultra chemiluminescent substrate (Pierce) on X-ray film (Agfa).

RESULTS

Design of High-Affinity TRAIL–Death Receptor Complexes. Several crystal structures of TRAIL in complex with the DR5 receptor are available (26, 31, 32), while the crystal structure of TRAIL in complex with the DR4 receptor is still not determined. Consequently, a TRAIL-DR4 homology model was constructed based on the crystal structure of the TRAIL-DR5–receptor complex with PDB coordinates 1D4V (26) as described before (19, 25). We previously validated the constructed TRAIL-DR4 model and the FoldX design process with experimentally available mutant data (19, 25). The TRAIL-DR5 and TRAIL-DR4 structural models were used in the FoldX design process to screen the receptor binding interface of TRAIL for single amino acid substitutions that would increase the affinity for the DR4 receptor (decreasing interaction energy ($\Delta\Delta G_i$)) in concert with an increased or unchanged affinity for DR5.

The FoldX *in silico* screening of the TRAIL receptor binding interface yielded several amino acid positions and (single) amino acid substitutions for enhancement of DR4 and DR5 binding affinity. From this screen, a mutant with a single amino acid replacement of glycine at position 131 to arginine appeared to be of particular interest. This variant was predicted to have increased affinity for both DR4 and DR5. Mutating to Lys instead of Arg was predicted to be less favorable, showing a smaller increase in affinity for DR4 and unchanged affinity for DR5 (Figure 1A). Models of TRAIL in complex with DcR1 and DcR2 were constructed, and the effect of the G131R and G131K mutations on binding affinity toward decoy receptors 1 and 2 was assessed. These

models predicted both G131R and G131K to increase or maintain the binding affinity of TRAIL toward DcR1 and DcR2.

Structural Basis for the Changes in Affinity. In the TRAIL-DR5 crystal structure (PDB coordinates 1D4V) Gly-131 is located at the N-terminal part of the AA' loop between two arginines (Arg-130 and Arg-132), and its C α is in close proximity to C γ and C δ of Arg-118 of the DR5 receptor (Figure 1B,C). The side chain conformation of Arg-118 is stabilized through an intrachain hydrogen bond interaction with Gln-101 of the receptor. The equivalent position to Arg-118 of DR5 in the DR4 receptor is Ala-169 (and Gln-101 of DR5 is Val-152 in DR4), and compared to the TRAIL-DR5 complex, this results in a pocket around position Gly-131 in the TRAIL-DR4 complex. Structural alignment of individual TRAIL and DR5 receptors present in the asymmetric crystal cell units from available crystal structures of TRAIL-DR5 complexes (1D4V, 1D0G, and 1DU3, respectively) reveals considerable structural heterogeneity in the region surrounding residue Gly-131 (Figure 1C). The AA' loop is very flexible, and the position of the Gly-131 C α in 1D0G and 1DU3 differs up to 8 Å when compared to the C α position in 1D4V, and the side chain of Arg-118 of DR5 also shows a wide range of conformations. For the design process the highest resolution structure of a TRAIL-DR5 complex (1D4V) was used as a template, and this structure is also the only that has a complete AA' loop. The ϕ , ψ angles of Gly-131 are within the allowed region of the Ramachandran plot.

Upon mutating Gly-131 to Arg, the Arg-131 side chain in the G131R-DR4 complex forms an intermolecular hydrogen bond in the G131R-DR4 complex bond with the main chain oxygen of Gly-151 of DR4 and partially fills the pocket (Figure 2B). In the G131R-DR5 complex, the side chain of Arg-118 moves out of the interface, and Arg-131 establishes a double interchain hydrogen bond with the Gly-100 main chain oxygen of DR5 and fills up the pocket (Figure 2A). In the case of the G131K substitution, the Arg-118 side chain of DR5 moves out of the interface as well, and in both DR4 and DR5 complexes Lys-131 occupies the pocket (Figure 2). In contrast to the G131R substitution, G131K does not seem to establish any hydrogen bond interaction with residues from the DR4 or DR5 receptor. In opposition to what might be expected from creating a highly charged patch on the surface of TRAIL (Arg-130, Arg/Lys-131, Arg-132) by substituting Gly-131 with Arg or Lys, the contribution of electrostatics to the gain in interaction energy is negligible. Decomposing the FoldX interaction energy term reveals that rather hydrophobic solvation and an increase in van der Waals interactions account for most of the gain in interaction energy. The gain in interaction energy due to hydrogen bond formation of Arg-131 with the DR4 and DR5 receptors is almost completely counterbalanced because of a large entropic penalty. However, the ability to participate in hydrogen bond formation with the DR4 and DR5 receptors causes the G131R variant to be slightly more favorable than the G131K variant. As can be appreciated from Figure 1C the conformational freedom of Arg-118 of the DR5 receptor is considerable; the entropic cost of forcing this Arg-118 into another conformation(s) is one of the main reasons for the predicted increase in affinity of G131R and G131K variants for DR4 compared to DR5.

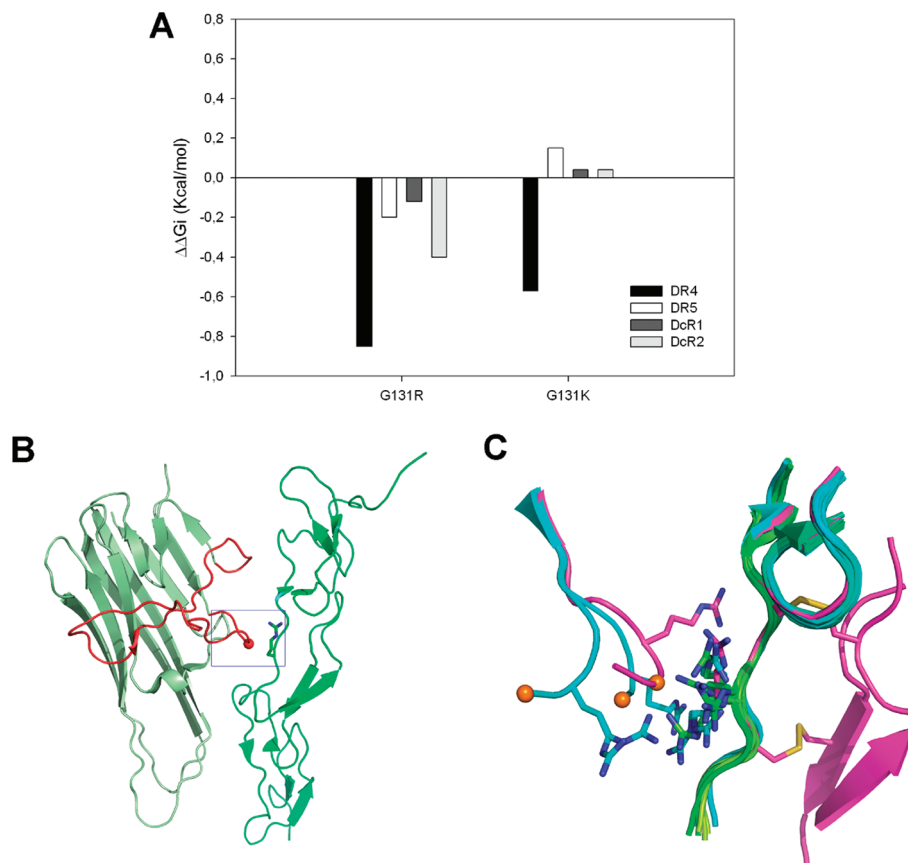


FIGURE 1: Binding energy predictions and structural overview of area surrounding Gly-131. (A) Predicted difference in binding energy ($\Delta\Delta G$) of Gly-131 variants binding to different death receptors when compared with wild-type rhTRAIL as determined by FoldX. The change in energy is measured in kcal/mol and applies to the change of a single binding interface bound to a single receptor. A negative $\Delta\Delta G_i$ indicates an improvement in receptor binding, and a positive $\Delta\Delta G_i$ indicates a decrease in receptor binding. (B) Ribbon drawing of a monomer TRAIL subunit (114–281) and DR5 monomer showing the various β strands and loops and the location of position G131 (blue box). (C) Structure heterogeneity around position 131 between different monomer TRAIL structures (left) and monomer DR5 structures (right) of known PDB coordinates for TRAIL or TRAIL-DR5 (PDB coordinates 1D0G in cyan, 1DU3 in green, and 1D4V in purple). Depicted are Arg130 of TRAIL and the C α of Gly-131 (orange sphere) together with Arg118 of the DR5 receptor.

The binding pocket of the DcR1 and DcR2 receptor is more similar to that of the DR4 than of the DR5 receptor: the positions equivalent to Gln-101 and Arg-118 in DR5 are valines in both DcR1 and DcR2 (data not shown). The absence of Arg in DcR1 and DcR2 at the position equivalent to Arg118 in DR5 results in no additional entropic cost upon mutation of Gly-131 toward Arg or Lys, thus resulting in interactions similar to the one observed in the TRAIL-DR4 complex.

Receptor Binding of rhTRAIL Variants. Binding of the purified ligands to immobilized DR4-Ig and DR5-Ig receptor chimeras was assessed in real time using surface plasmon resonance (SPR). Receptor binding curves were recorded using rhTRAIL concentrations ranging from 0.5 to 250 nM at 37 °C (Figure 3A,B). Apparent dissociation constants were calculated from pre-steady-state response values (Table 1). Data were fitted using a standard four-parameter equation. Both variants G131R and G131K showed ~ 3 - and ~ 1.7 -fold increase in apparent affinity for binding to DR4-Ig, respectively, mainly due to a higher association to the directly immobilized receptors DR4-Ig (Supporting Information Figure S2). The increase in affinity to DR5-Ig was slightly more modest with ~ 2.4 - and 1.5-fold increase in apparent affinity to immobilized DR5-Ig for G131R and G131K, respectively. ELISA assays confirmed the increase in affinity toward both death receptors. Receptor response curves were

recorded using rhTRAIL concentrations ranging from 0 to 1000 ng per well (Figure 3C,D), with both variants displaying an approximate 3-fold increase in affinity toward DR4 (Figure 3C, Table 1). Similarly to the SPR assay we observed for both variants a smaller increase in affinity for DR5 than for DR4 (Figure 3D, Table 1). An increase in apparent affinity was also observed to the decoy receptors DcR1- and DcR2-Ig as measured by SPR (Supporting Information Figure S3).

To assess the binding preference of the Gly-131 variants, a competitive ELISA assay was performed using coated DR4-Ig plates and competitive soluble receptors DR4-, DR5-, DcR1-, and DcR2-Ig (Figure 4). Soluble DR4-Ig was shown to be very efficient in reducing the binding of the variants G131R and G131K (by ~ 7 -fold) when compared to wild-type rhTRAIL (Figure 4A), indicating an increased affinity to soluble competitive DR4-Ig leading to a lower binding to immobilized DR4-Ig. Soluble DR5-Ig was less efficient than DR4-Ig in neutralizing binding of the Gly-131 variants, however, with a nearly similar competitive behavior as observed for wild-type rhTRAIL (Figure 4B). DcR1-Ig was also able to compete for binding of the variants to DR4-Ig with an almost 3-fold reduction in binding when compared with wild-type rhTRAIL (Figure 4C). A nearly equivalent ratio was observed for wild-type rhTRAIL and variants for DcR2-Ig competition to DR4-Ig binding, with the variants

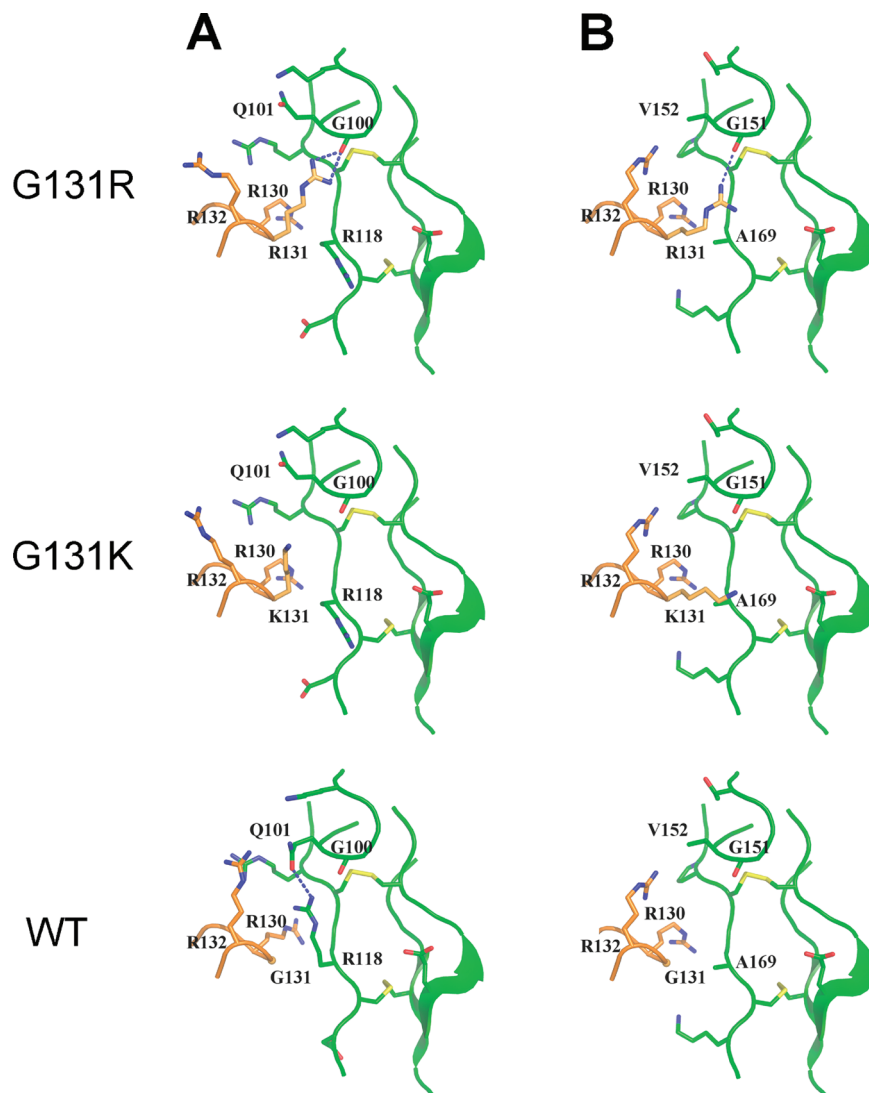


FIGURE 2: Structural impressions of the area around 131 for wild-type rhTRAIL and Gly-131 variants as determined by FoldX: (A) TRAIL-DR5 and (B) TRAIL-DR4.

showing a very small decrease in binding to soluble DcR2-Ig when compared with wild-type rhTRAIL (Figure 4D).

Taken together, these results indicate an increased affinity toward both death receptors DR4-Ig and DR5-Ig, with the highest increase observed for the lowest affinity death receptor DR4, confirming the prediction trend between DR4 and DR5 given by FoldX.

Biological Activity: Apoptotic Potential of rhTRAIL Variants in Cancer Cells. To examine the apoptotic potential of the G131 variants, a broad range of cell lines in which the TRAIL-death signal is transmitted by DR4, DR5, or both was tested. The sensitivity toward Gly-131 variants was assessed by comparing cell death induced by wild-type rhTRAIL and Gly-131 variants. Burkitt's lymphoma wild-type BJAB cells responsive to both DR4- and DR5-mediated cell death (BJAB^{WT}) and BJAB cells deficient in DR5 (BJAB^{DR5 DEF}) (33) were tested first (Figure 5). In combination with 0.33 μ g/mL cycloheximide, the variants G131R and G131K were able to induce an \sim 3-fold increase in cell death relative to wild-type rhTRAIL in wild-type BJAB cells (Figure 5A, Table 2). BJAB^{DR5 DEF} cells displayed markedly lower sensitivity to wild-type rhTRAIL, with a reduction in maximum cell death from 91% for wild-type BJAB to only 25% maximum cell death for the BJAB^{DR5 DEF} cell line

(Figure 5B, Table 2). The Gly-131 variants retained a higher efficiency on the BJAB^{DR5 DEF} cell lines with a substantially augmented cell death induction (60% maximum cell death) when compared to wild-type rhTRAIL. In the absence of cycloheximide the Gly-131 variants were able to efficiently augment cell death in BJAB^{WT} cell lines, reaching a maximum cell death induction of 56% against a maximum cell death induction of 36% for rhTRAIL WT (Figure 5C). No significant *in vitro* killing could be monitored using the same conditions for BJAB^{DR5 DEF} cells.

Study in colon carcinoma cell lines Colo205 and SW948 also showed that the mutants were able to induce significantly higher levels of cell death than wild-type rhTRAIL (Figure 6A,B). In Colo205 cells both DR4 and DR5 are functional, although in Colo205 cells DR5 is the predominant mediator of the TRAIL-death signal (19). In contrast, in SW948 cells DR4 is the major mediator of TRAIL-induced apoptosis (34). As seen in Figure 6A,B, the Gly-131 variants could enhance cell death in both DR4- and DR5-sensitive colon carcinoma cell lines. The EC₅₀ values and maximum cell death achieved by the variants versus wild-type rhTRAIL are listed in Table 2. Analysis of caspase (DEVDase) activity in SW948 cells showed a higher caspase activity induced by the Gly-131 variants (100 ng/mL) compared to wild-type rhTRAIL,

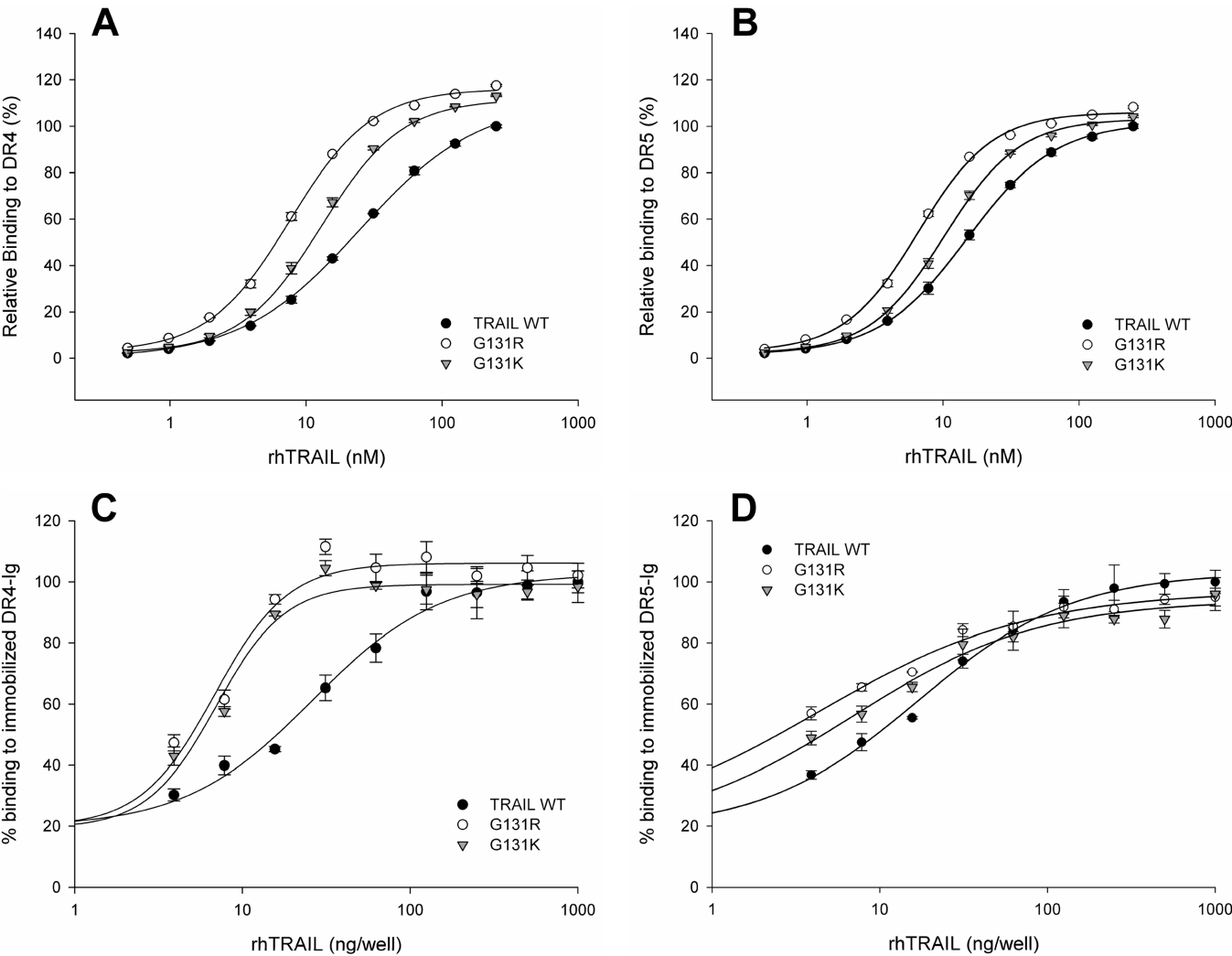


FIGURE 3: Receptor binding of wild-type rhTRAIL and Gly-131 variants as determined by SPR and ELISA. Receptor binding of wild-type rhTRAIL, G131R, and G131K to DR4-Ig as determined by SPR (A) or to DR5-Ig (B). To obtain pre-steady-state data that represent proper high-affinity complex formation, and assuming the initial fast off-rate to represent lower complexes, the response at each concentration was recorded 30 s after the end of the injections. Receptor binding was calculated relative to the response of wild-type rhTRAIL at 250 nM. (C) Receptor binding of wild-type rhTRAIL, G131R, and G131K to DR4-Ig as determined by ELISA or to DR5-Ig (D).

Table 1: Apparent DR4 and DR5 Binding Affinities of Wild-Type rhTRAIL, G131R, and G131K As Determined Using a Pre-Steady-State Approach by SPR and ELISA^a

protein	SPR		ELISA	
	app K_D (nM), DR4	app K_D (nM), DR5	app K_D (nM), DR4	app K_D (nM), DR5
rhTRAIL WT	24.9 (± 1.2)	17.8 (± 1.8)	3.8 (± 0.3)	2.5 (± 0.2)
G131R	8.7 (± 1.0)	7.9 (± 1.3)	1.2 (± 0.5)	0.9 (± 0.4)
G131K	15.0 (± 1.5)	12.3 (± 1.8)	1.4 (± 0.3)	1.2 (± 0.3)

^a Apparent K_D 's were calculated using a four-parameter curve fitting tool.

confirming the stronger agonistic potential of the mutants (Figure 6C). In addition, HCT15 colon carcinoma, HepG2 hepatocellular carcinoma, and BxPC pancreatic carcinoma cells were examined (Figure 6D). On colon carcinoma HCT15 cells the Gly-131 were more effective only at low concentrations (5 and 10 ng/mL), whereas a similar apoptotic potential was observed at higher concentrations (Figure 6) (Supporting Information Figure S6). HepG2 cell type was the only cell type that did not display higher levels of apoptosis in comparison to rhTRAIL WT, whereas a significantly higher proapoptotic potential in BxPC cell lines

was observed in comparison to wild-type rhTRAIL in almost all concentrations tested (Figure 6D).

ML-1 and EM-2 are acute myeloid leukemia and chronic myeloid leukemia cell lines, respectively, both cell lines solely DR4-responsive (19) (Figure 7A,B). The Gly-131 variants displayed a significantly higher proapoptotic potential in both leukemia cell lines in comparison to wild-type rhTRAIL. Supporting these results, in ML-1 cells G131R and G131K (100 ng/mL) induced a stronger processing of caspase-3 to its active p19/17 large subunits than wild-type rhTRAIL (100 ng/mL) (Supporting Information Figure S4). Processing of caspase-3 induced by G131R and G131K correlated with a higher percentage of cells with externalized phosphatidylserine compared to wild-type rhTRAIL (Supporting Information Figure S4). Pretreatment with the pan-caspase inhibitor of z-VAD.fmk (10 μ M) almost completely prevented phosphatidylserine exposure and formation of the p19/17 large subunits, confirming the induction of a caspase-dependent apoptotic pathway.

Moreover, the variants were tested for activity on normal cells, namely, human nontransformed fibroblasts (hFB) from two different donors and human umbilical endothelial

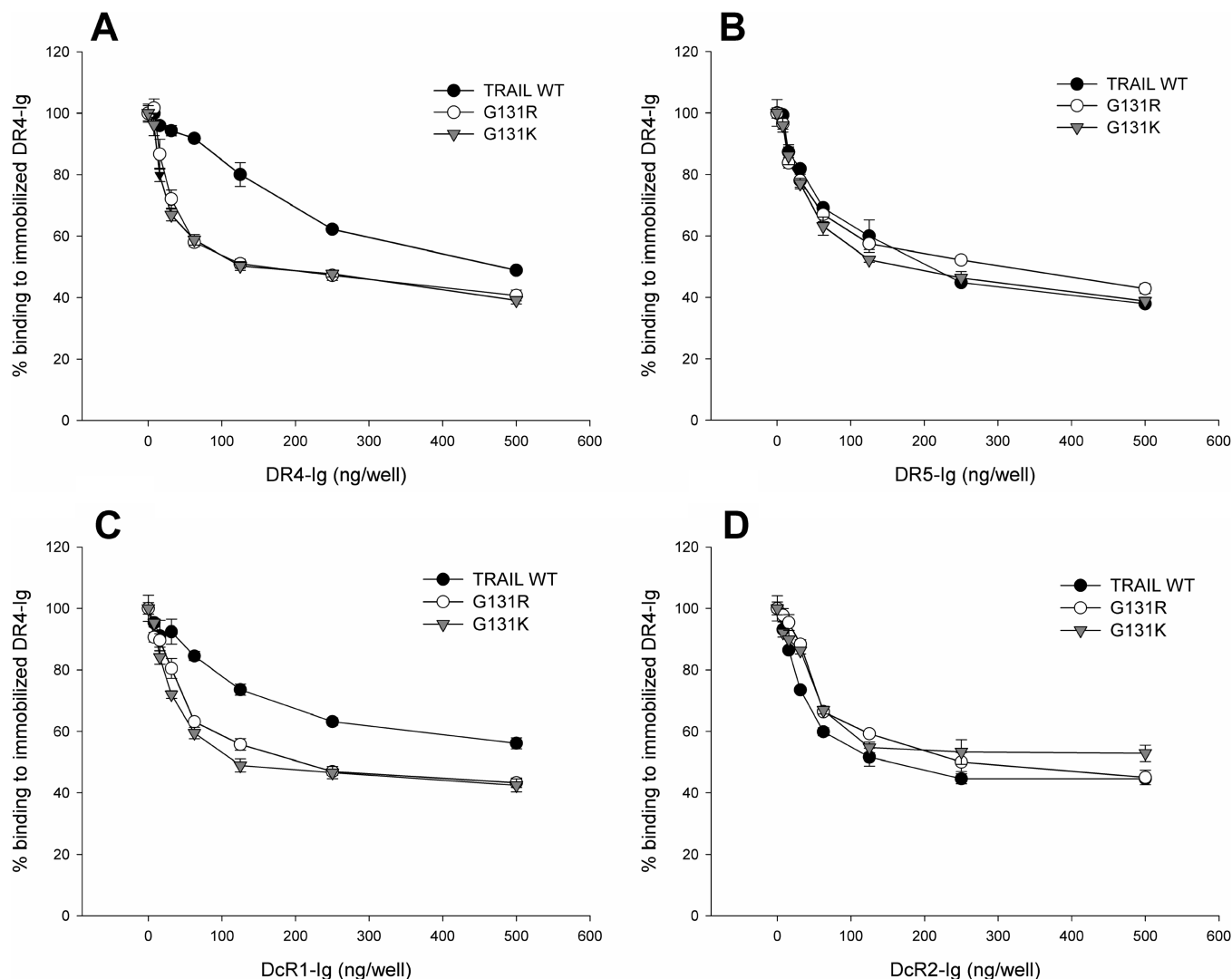


FIGURE 4: Competitive ELISA by TRAIL receptors of wild-type TRAIL and Gly-131 variants binding to immobilized DR4-Ig receptor using (A) soluble DR4-Ig as competitor, (B) soluble DR5-Ig as competitor, (C) soluble DcR1-Ig as competitor, or (D) soluble DcR2-Ig as competitor. Ten nanograms per well of wild-type rhTRAIL or Gly-131 variants was preincubated with 0–500 ng per well of DR4, DR5-Ig, DcR1-Ig, or DcR2-Ig for 1 h. Preincubated solutions were added to microtiter plates coated with DR4-Ig. Binding of the selective variants at various concentrations of soluble receptor toward the immobilized DR4-Ig was calculated relative to the value measured on the presence of 0 ng per well of soluble receptor.

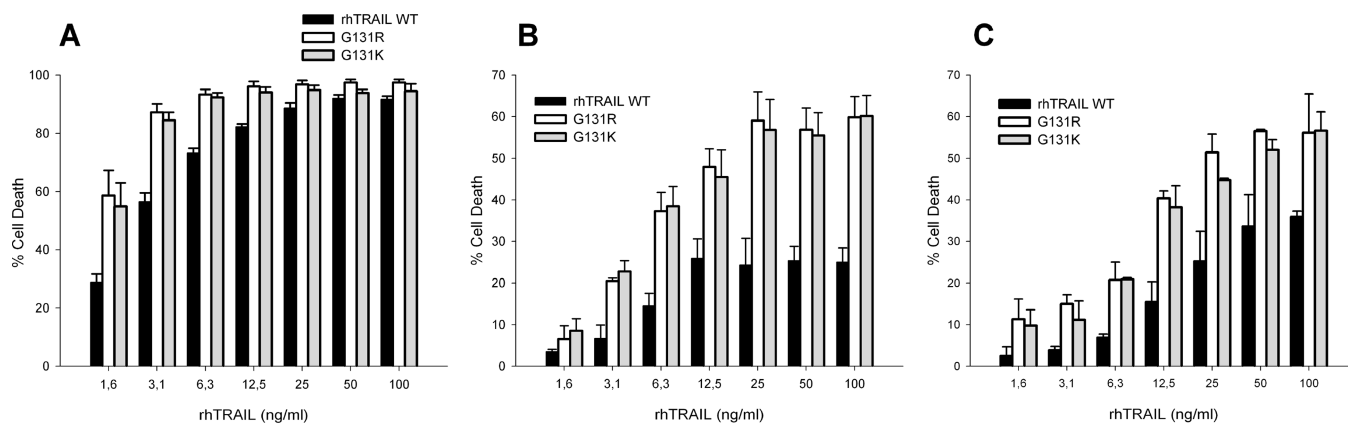


FIGURE 5: Cytotoxic potential (% cell death) of wild-type rhTRAIL or Gly-131 variants in BJAB cells responsive to both DR4- and DR5-mediated cell death (BJAB^{WT}) relative to cycloheximide control (0.33 μ g/mL) (A), BJAB cells deficient for DR5 (BJAB^{DR5 DEF}) relative to cycloheximide control (0.33 μ g/mL) (B), and BJAB WT without cycloheximide (C). Cells were treated with wild-type rhTRAIL and Gly-131 variants or buffer control for 24 h. The percentage of cell death was calculated relative to the control wells containing no ligand. The data are the mean \pm SEM of two independent experiments in triplicate.

Table 2: EC₅₀ Values for BJAB WT, BJAB DR5 Deficient, Colo205, and SW948 cells^a

protein	BJAB ^{WT}		BJAB ^{DR5 DEF}		Colo205		SW948	
	EC ₅₀ (ng/mL)	max effect % cell death	EC ₅₀ (ng/mL)	max effect % cell death	EC ₅₀ (ng/mL)	max effect % cell death	EC ₅₀ (ng/mL)	max effect % cell death
rhTRAIL	2.8 ± 0.8	91 ± 2	5.48 ± 4	25 ± 3	9.8 ± 2.1	89.5 ± 5	11.9 ± 2.8	45 ± 2
G131R	1.0 ± 0.6	97 ± 3	4.7 ± 1.3	60 ± 4	6.1 ± 2.5	90.9 ± 4	8.15 ± 1.1	61 ± 4
G131K	1.1 ± 0.8	94 ± 3	4.4 ± 1.0	60 ± 5	7.5 ± 3.1	92.0 ± 4	7.0 ± 1.5	57 ± 3

^a BJAB WT and BJAB DR5 deficient cells were treated in combination with 0.33 μg/mL cycloheximide. EC₅₀ values were calculated using a four-parameter curve fitting tool.

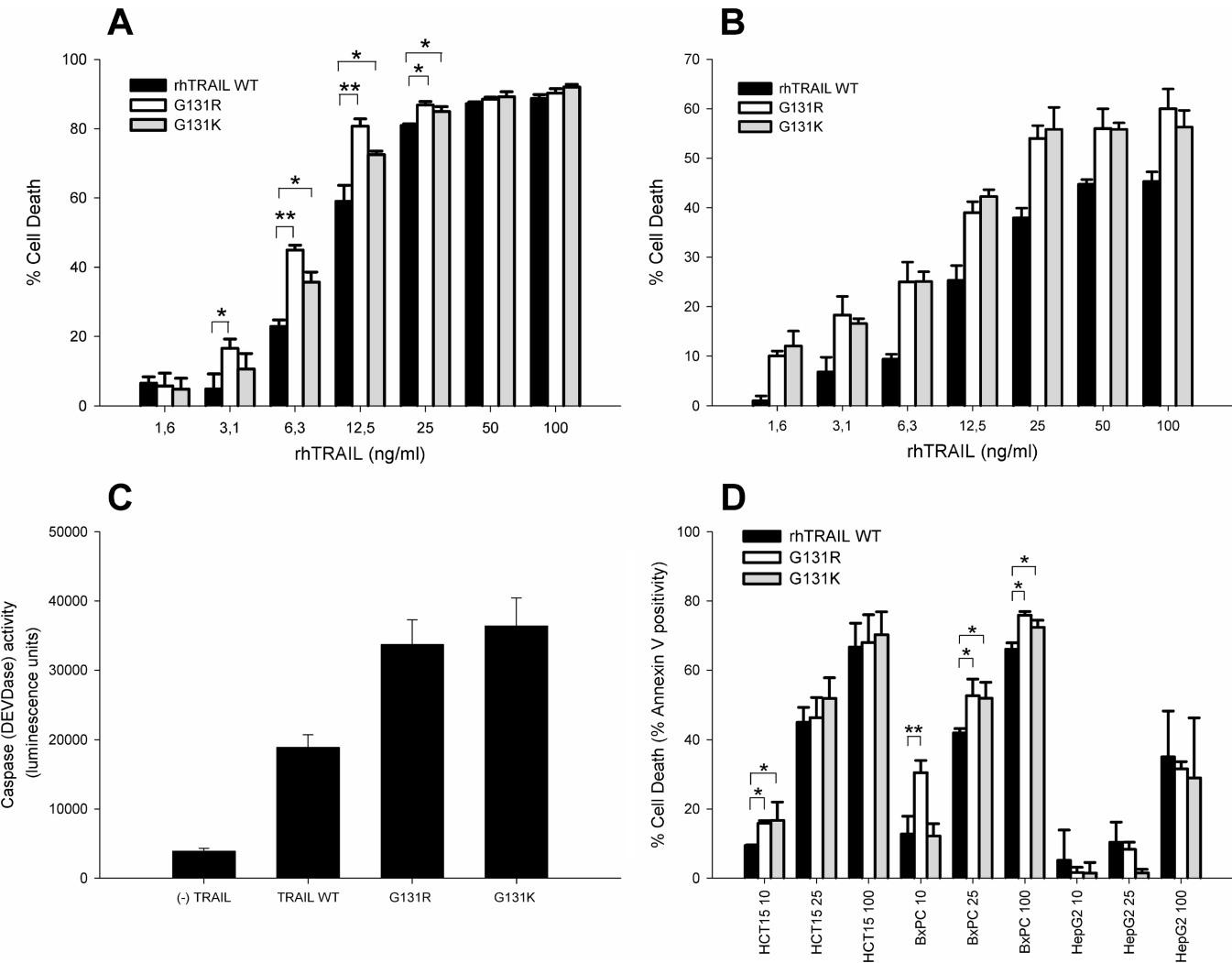


FIGURE 6: Sensitivity enhancement of cancer cell lines to TRAIL-induced apoptosis by Gly-131 variants on several cancer cell lines. Shown is the cytotoxic potential (% cell death) of wild-type rhTRAIL or Gly-131 variants in Colo205 colon carcinoma DR5 mediated cell line (A) and SW948 colon carcinoma DR4 mediated cell line (B). Cells were treated with wild-type rhTRAIL and Gly-131 variants or buffer control for 24 h. The percentage of cell death was calculated relative to the control wells containing no ligand. (C) Caspase (DEVDase) activity by wild-type rhTRAIL and variants G131R and G131K (100 ng/mL) after 20 h of treatment as measured by luminescence on SW948 cell lines. Apoptosis-inducing activity (annexin V staining) of wild-type rhTRAIL or Gly-131 variants in HCT15 colon carcinoma, BxPC pancreatic carcinoma, and HepG2 hepatocellular carcinoma (10, 25, and 100 ng/mL) (D). The results are mean values ± SEM (*n* = 3). Asterisks denote statistically significant differences (*, *P* < 0.05; **, *P* < 0.001) between the indicated pairs.

(HUVEC) cells. There was no significant difference in the response of the two donor hFB cell cultures. Neither of the Gly-131 variants nor rhTRAIL WT displayed significant activity on the cell lines studied, indicating that the increase in apoptotic activity had no effect on normal cells (Figure 7C,D).

Interestingly, a time-dependent incubation of ML-1 cells with the Gly-131 variants resulted in a faster caspase-8 activation, underlining their increased apoptotic activity (Supporting Information Figure S5).

Taken together, these results demonstrate that, by affinity enhancement primarily toward the death receptor 4, our variants could significantly potentiate the apoptotic property of TRAIL in a wide range of tumor cell lines.

DISCUSSION

TRAIL interacts with five receptors of the TNF-R family; however, only receptors DR4 and DR5 are able to induce apoptosis. From these two death receptors DR5 is the highest

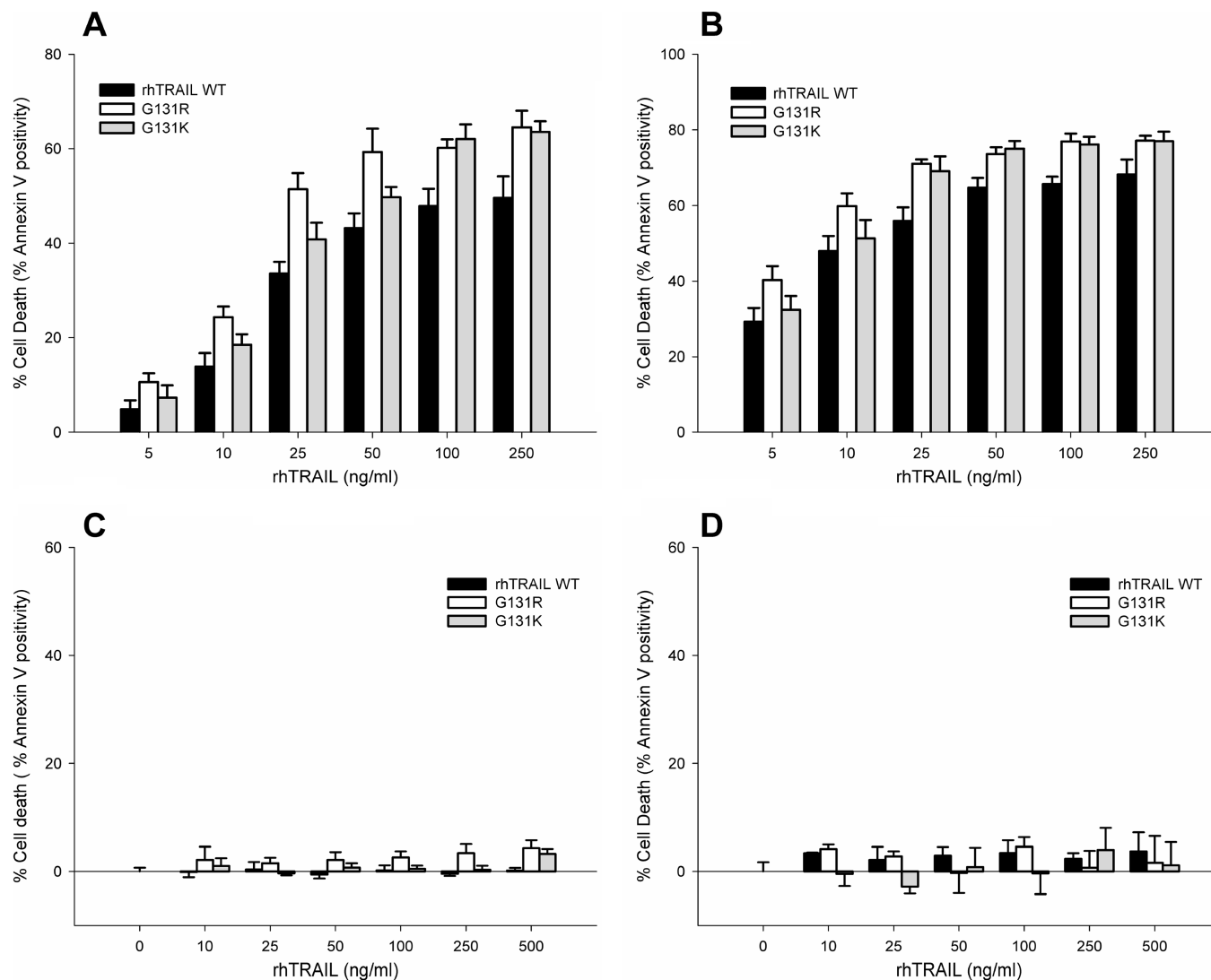


FIGURE 7: Apoptosis-inducing activity (annexin V staining) of wild-type rhTRAIL or Gly-131 variants in ML-1 chronic myeloid leukemia DR4 mediated cell line (A), EM-2 chronic myeloid leukemia DR4 mediated cell line (B), human umbilical vein endothelial cells (HUVEC) (C), and human primary, nontransformed fibroblasts (hFB) from two different donors (D). Cells were treated with the indicated concentrations of rhTRAIL WT, G131K, or G131R for 24 h after which induction of cell death was quantified with annexin V staining. The graph shows average percentage death induced \pm SEM.

affinity receptor (18, 19, 25) and the primary receptor leading to apoptosis. The difference in affinity for DR4 and DR5 may be a mechanism by which some cancer cells are more sensitive toward DR5-TRAIL-induced apoptosis.

As certain tumor cell lines appear to be only sensitive to DR4-mediated apoptosis, in particular certain leukemia and lymphoma tumors, and many other tumor cells are responsive to both DR4- and DR5-mediated apoptosis, we decided to design agonistic TRAIL variants by primarily increasing the affinity toward DR4 without drastically altering the affinity for DR5 and therefore increasing the general apoptotic potential of rhTRAIL.

Several DR4- and DR5-selective TRAIL variants have been developed in recent years using various methodologies: by using computational design (19, 25), by employing directed evolution (16), or by a rational approach (21). The DR5-selective TRAIL variants have an increased affinity toward DR5 and significantly increased biological activity in appropriate DR5-sensitive cell lines when compared to wild-type rhTRAIL. In contrast, all previously developed DR4-selective TRAIL variants show a significantly reduced

biological activity when compared to wild-type rhTRAIL. While the DR4-selective variant obtained by directed evolution showed an \sim 2-fold decrease in affinity for DR4 as measured by SPR (16), it was shown to be largely inactive in DR4-responsive Ramos cells (21). Changing one of the six amino acid mutations of this variant back to wild type restored biological activity although still being lower than wild-type rhTRAIL (21). In comparison, the DR4-selective variant generated by our group using computational protein design retained its affinity for the DR4 receptor with only small reduction of its proapoptotic potential (25). Nevertheless, at lower protein concentrations, all of the previously designed DR4-selective TRAIL variants were less active than wild-type rhTRAIL.

Therefore, in order to generate a TRAIL variant that is able to induce apoptosis more efficiently through DR4, we decided to focus on mutations that primarily improve the affinity toward DR4 and less on receptor specificity. The protein design algorithm FoldX identified in an *in silico* screen TRAIL G131R and G131K substitutions as promising ones in achieving this goal. Position 131 of TRAIL has not

been identified before as being important for receptor binding by the alanine scanning or phage display experiments (16, 32).

Receptor binding experiments using SPR, ELISA, and competitive ELISA confirmed the design predictions, showing the highest gain in affinity for DR4 and a more modest affinity enhancement for DR5. It also confirmed that from the two variants constructed the G131R variant displayed the higher affinity for DR4 and DR5. The observed increase in affinity by mutations G131R and G131K for DcR1 and DcR2 is in accordance with the similar structural environment around position 131 as observed in TRAIL-DR4, TRAIL-DcR1, and TRAIL-DcR2 complexes. The absence of an Arg at the position equivalent to position 118 in DR5 explains why G131R and G131K have a higher affinity for DR4 and both of the decoy receptors than for DR5.

The G131R and G131K variants showed enhanced apoptosis-inducing activity in cell line assays. In both DR4- and DR5-responsive tumor cells, G131R and G131K variants showed a higher proapoptotic activity when compared to wild-type rhTRAIL. However, this effect was more pronounced in cells mainly responsive to DR4-mediated cell death. The increased maximum apoptotic activity of the variants in these cell lines suggests a clinical interest for these variants. Interestingly, although the G131R and G131K mutations also increased the affinity of TRAIL for DcR1 and DcR2 with the same magnitude as for DR4, this appears not to be important for the proapoptotic activity on the panel of cell lines tested. Given the reported differences in the affinity between decoy receptors and death-inducing TRAIL receptors (TRAIL has higher affinity toward the death-inducing receptors), at low concentrations TRAIL or the G131 variants probably preferentially bind to the death-inducing receptors and only at higher ligand concentrations do the decoy receptors get occupied. Due to this apparent, nonlinear correlation between decoy and death receptor expression and affinity, we hypothesize that the proapoptotic activity of TRAIL can be improved by simply improving its affinity for the death-inducing receptors (DR4, DR5) even if the affinity for decoy receptors also improves. Taken together, our designed variants show an enhanced apoptosis-inducing activity mediated through DR5 and, even more potently, through DR4.

In conclusion, these results show that it is possible to introduce new variations in rhTRAIL that significantly enhance its antitumor properties by increasing the affinity toward its death-inducing receptors.

ACKNOWLEDGMENT

We thank Dr. Andrew Thorburn (University of Colorado Health Sciences Center, Aurora, CO) for kindly providing the BJAB cell lines and Dr. Steven de Jong (University Medical Center, Groningen, The Netherlands) for providing the SW948 cell line and Francois Stricher (CRG, Barcelona) for helpful discussions regarding TRAIL design.

SUPPORTING INFORMATION AVAILABLE

Six figures which describe the gel filtration profile of variants constructed by mutagenesis, SPR sensorgrams for the death receptors, decoy receptor pre-steady-state curves, caspase-3 and caspase-8 activation in ML-1 cells, and apoptotic activity of variants on HCT15 and BxPc cells. This

material is available free of charge via the Internet at <http://pubs.acs.org>.

REFERENCES

- Ashkenazi, A. (2008) Targeting the extrinsic apoptosis pathway in cancer. *Cytokine Growth Factor Rev.* 19, 325–331.
- Ashkenazi, A., Pai, R. C., Fong, S., Leung, S., Lawrence, D. A., Marsters, S. A., Blackie, C., Chang, L., McMurtrey, A. E., Hebert, A., DeForge, L., Koumenis, I. L., Lewis, D., Harris, L., Bussiere, J., Koeppen, H., Shahrokh, Z., and Schwall, R. H. (1999) Safety and antitumor activity of recombinant soluble Apo2 ligand. *J. Clin. Invest.* 104, 155–162.
- Lawrence, D., Shahrokh, Z., Marsters, S., Achilles, K., Shih, D., Mounho, B., Hillan, K., Totpal, K., DeForge, L., Schow, P., Hooley, J., Sherwood, S., Pai, R., Leung, S., Khan, L., Gliniak, B., Bussiere, J., Smith, C. A., Strom, S. S., Kelley, S., Fox, J. A., Thomas, D., and Ashkenazi, A. (2001) Differential hepatocyte toxicity of recombinant Apo2L/TRAIL versions. *Nat. Med.* 7, 383–385.
- LeBlanc, H. N., and Ashkenazi, A. (2003) Apo2L/TRAIL and its death and decoy receptors. *Cell Death Differ.* 10, 66–75.
- Chaudhary, P. M., Eby, M., Jasmin, A., Bookwalter, A., Murray, J., and Hood, L. (1997) Death receptor 5, a new member of the TNFR family, and DR4 induce FADD-dependent apoptosis and activate the NF-kappaB pathway. *Immunity* 7, 821–830.
- Kuang, A. A., Diehl, G. E., Zhang, J., and Winoto, A. (2000) FADD is required for DR4- and DR5-mediated apoptosis: lack of trail-induced apoptosis in FADD-deficient mouse embryonic fibroblasts. *J. Biol. Chem.* 275, 25065–25068.
- Schneider, P., Thome, M., Burns, K., Bodmer, J. L., Hofmann, K., Kataoka, T., Holler, N., and Tschopp, J. (1997) TRAIL receptors 1 (DR4) and 2 (DR5) signal FADD-dependent apoptosis and activate NF-kappaB. *Immunity* 7, 831–836.
- Bodmer, J. L., Holler, N., Reynard, S., Vinciguerra, P., Schneider, P., Juo, P., Blenis, J., and Tschopp, J. (2000) TRAIL receptor-2 signals apoptosis through FADD and caspase-8. *Nat. Cell Biol.* 2, 241–243.
- Kischkel, F. C., Lawrence, D. A., Chuntharapai, A., Schow, P., Kim, K. J., and Ashkenazi, A. (2000) Apo2L/TRAIL-dependent recruitment of endogenous FADD and caspase-8 to death receptors 4 and 5. *Immunity* 12, 611–620.
- Sprick, M. R., Weigand, M. A., Rieser, E., Rauch, C. T., Juo, P., Blenis, J., Krammer, P. H., and Walczak, H. (2000) FADD/MORT1 and caspase-8 are recruited to TRAIL receptors 1 and 2 and are essential for apoptosis mediated by TRAIL receptor 2. *Immunity* 12, 599–609.
- Kimberley, F. C., and Screaton, G. R. (2004) Following a TRAIL: update on a ligand and its five receptors. *Cell Res.* 14, 359–372.
- Clancy, L., Mruk, K., Archer, K., Woelfel, M., Mongkolsapaya, J., Screaton, G., Lenardo, M. J., and Chan, F. K. (2005) Preligand assembly domain-mediated ligand-independent association between TRAIL receptor 4 (TR4) and TR2 regulates TRAIL-induced apoptosis. *Proc. Natl. Acad. Sci. U.S.A.* 102, 18099–18104.
- Merino, D., Lalaoui, N., Morizot, A., Schneider, P., Solary, E., and Micheau, O. (2006) Differential inhibition of TRAIL-mediated DR5-DISC formation by decoy receptors 1 and 2. *Mol. Cell. Biol.* 26, 7046–7055.
- Ichikawa, K., Liu, W., Zhao, L., Wang, Z., Liu, D., Ohtsuka, T., Zhang, H., Mountz, J. D., Koopman, W. J., Kimberly, R. P., and Zhou, T. (2001) Tumoricidal activity of a novel anti-human DR5 monoclonal antibody without hepatocyte cytotoxicity. *Nat. Med.* 7, 954–960.
- Almasan, A., and Ashkenazi, A. (2003) Apo2L/TRAIL: apoptosis signaling, biology, and potential for cancer therapy. *Cytokine Growth Factor Rev.* 14, 337–348.
- Kelley, R. F., Totpal, K., Lindstrom, S. H., Mathieu, M., Billeci, K., DeForge, L., Pai, R., Hymowitz, S. G., and Ashkenazi, A. (2005) Receptor-selective mutants of apoptosis-inducing ligand 2/tumor necrosis factor-related apoptosis-inducing ligand reveal a greater contribution of death receptor (DR) 5 than DR4 to apoptosis signaling. *J. Biol. Chem.* 280, 2205–2212.
- Szegezdi, E., Cahill, S., Meyer, M., O'Dwyer, M., and Samali, A. (2006) TRAIL sensitisation by arsenic trioxide is caspase-8 dependent and involves modulation of death receptor components and Akt. *Br. J. Cancer* 94, 398–406.
- Truneh, A., Sharma, S., Silverman, C., Khandekar, S., Reddy, M. P., Deen, K. C., McLaughlin, M. M., Srinivasula, S. M., Livi,

- G. P., Marshall, L. A., Alnemri, E. S., Williams, W. V., and Doyle, M. L. (2000) Temperature-sensitive differential affinity of TRAIL for its receptors. DR5 is the highest affinity receptor. *J. Biol. Chem.* 275, 23319–23325.
19. van der Sloot, A. M., Tur, V., Szegezdi, E., Mullally, M. M., Cool, R. H., Samali, A., Serrano, L., and Quax, W. J. (2006) Designed tumor necrosis factor-related apoptosis-inducing ligand variants initiating apoptosis exclusively via the DR5 receptor. *Proc. Natl. Acad. Sci. U.S.A.* 103, 8634–8639.
20. MacFarlane, M., Inoue, S., Kohlhaas, S. L., Majid, A., Harper, N., Kennedy, D. B., Dyer, M. J., and Cohen, G. M. (2005) Chronic lymphocytic leukemic cells exhibit apoptotic signaling via TRAIL-R1. *Cell Death Differ.* 12, 773–782.
21. MacFarlane, M., Kohlhaas, S. L., Sutcliffe, M. J., Dyer, M. J., and Cohen, G. M. (2005) TRAIL receptor-selective mutants signal to apoptosis via TRAIL-R1 in primary lymphoid malignancies. *Cancer Res.* 65, 11265–11270.
22. Kortemme, T., Joachimiak, L. A., Bullock, A. N., Schuler, A. D., Stoddard, B. L., and Baker, D. (2004) Computational redesign of protein-protein interaction specificity. *Nat. Struct. Mol. Biol.* 11, 371–379.
23. Reina, J., Lacroix, E., Hobson, S. D., Fernandez-Ballester, G., Rybin, V., Schwab, M. S., Serrano, L., and Gonzalez, C. (2002) Computer-aided design of a PDZ domain to recognize new target sequences. *Nat. Struct. Biol.* 9, 621–627.
24. Shifman, J. M., and Mayo, S. L. (2002) Modulating calmodulin binding specificity through computational protein design. *J. Mol. Biol.* 323, 417–423.
25. Tur, V., van der Sloot, A. M., Reis, C. R., Szegezdi, E., Cool, R. H., Samali, A., Serrano, L., and Quax, W. J. (2008) DR4 selective TRAIL variants obtained by structure based design. *J. Biol. Chem.* 29, 20560–20568.
26. Mongkolsapaya, J., Grimes, J. M., Chen, N., Xu, X. N., Stuart, D. I., Jones, E. Y., and Screaton, G. R. (1999) Structure of the TRAIL-DR5 complex reveals mechanisms conferring specificity in apoptotic initiation. *Nat. Struct. Biol.* 6, 1048–1053.
27. Guerois, R., Nielsen, J. E., and Serrano, L. (2002) Predicting changes in the stability of proteins and protein complexes: a study of more than 1000 mutations. *J. Mol. Biol.* 320, 369–387.
28. Schymkowitz, J. W., Rousseau, F., Martins, I. C., Ferkinghoff-Borg, J., Stricher, F., and Serrano, L. (2005) Prediction of water and metal binding sites and their affinities by using the Fold-X force field. *Proc. Natl. Acad. Sci. U.S.A.* 102, 10147–10152.
29. Hymowitz, S. G., O'Connell, M. P., Ultsch, M. H., Hurst, A., Totpal, K., Ashkenazi, A., de Vos, A. M., and Kelley, R. F. (2000) A unique zinc-binding site revealed by a high-resolution X-ray structure of homotrimeric Apo2L/TRAIL. *Biochemistry* 39, 633–640.
30. van der Sloot, A. M., Mullally, M. M., Fernandez-Ballester, G., Serrano, L., and Quax, W. J. (2004) Stabilization of TRAIL, an all-beta-sheet multimeric protein, using computational redesign. *Protein Eng. Des. Sel.* 17, 673–680.
31. Cha, S. S., Sung, B. J., Kim, Y. A., Song, Y. L., Kim, H. J., Kim, S., Lee, M. S., and Oh, B. H. (2000) Crystal structure of TRAIL-DR5 complex identifies a critical role of the unique frame insertion in conferring recognition specificity. *J. Biol. Chem.* 275, 31171–31177.
32. Hymowitz, S. G., Christinger, H. W., Fuh, G., Ultsch, M., O'Connell, M., Kelley, R. F., Ashkenazi, A., and de Vos, A. M. (1999) Triggering cell death: the crystal structure of Apo2L/TRAIL in a complex with death receptor 5. *Mol. Cell* 4, 563–571.
33. Thomas, L. R., Johnson, R. L., Reed, J. C., and Thorburn, A. (2004) The C-terminal tails of tumor necrosis factor-related apoptosis-inducing ligand (TRAIL) and Fas receptors have opposing functions in Fas-associated death domain (FADD) recruitment and can regulate agonist-specific mechanisms of receptor activation. *J. Biol. Chem.* 279, 52479–52486.
34. van Geelen, C. M., de Vries, E. G., Le, T. K., van Weeghel, R. P., and de Jong, S. (2003) Differential modulation of the TRAIL receptors and the CD95 receptor in colon carcinoma cell lines. *Br. J. Cancer* 89, 363–373.

BI801927X